Supporting Information

Piatkov et al. 10.1073/pnas.1401639111

SI Text

Detailed (Extended) Legend to Fig. 1. The N-end rule pathway.

The main determinant of an N-degron is a destabilizing N-terminal residue of a protein. N-terminal residues are indicated by single-letter abbreviations for amino acids. A yellow oval denotes the rest of a protein substrate. Recognition components of the N-end rule pathway are called N-recognins.

Regulated degradation of proteins or their fragments by the N-end rule pathway mediates a strikingly broad range of biological functions, including the sensing of heme, nitric oxide, oxygen, and short peptides; the control, through subunit-selective degradation, of the input stoichiometries of subunits in oligomeric protein complexes; the elimination of misfolded or otherwise abnormal proteins; the degradation of specific proteins after their retrotranslocation to the cytosol from mitochondria or other membrane-enclosed compartments; the repression of apoptosis and neurodegeneration; the regulation of chromosome transcription, repair, replication, and cohesion/segregation; the regulation of G proteins, autophagy, peptide import, meiosis, immunity, fat metabolism, cell migration, actin filaments, cardiovascular development, spermatogenesis, neurogenesis, and memory; and the regulation of many processes in plants (1–59). In eukaryotes, the N-end rule pathway consists of two branches (*A* and *B*).

Part A. The Arg/N-end rule pathway: the prefix Arg in the pathway's name refers to N-terminal arginylation (Nt-arginylation) of N-end rule substrates, a significant feature of this system. The Arg/N-end rule pathway targets specific unacetylated N-terminal residues. In the yeast *S. cerevisiae*, the Arg/N-end rule pathway is mediated by the Ubr1 N-recognin, a 225-kDa RING-type E3 Ub ligase and a part of the targeting apparatus comprising a complex of the Ubr1-Rad6 and Ufd4-Ubc4/5 holoenzymes (1, 4, 9). In multicellular eukaryotes, several functionally overlapping E3 Ub ligases (Ubr1, Ubr2, Ubr4, and Ubr5) function as N-recognins of this pathway. An N-recognin binds to the primary destabilizing N-terminal residues Arg, Lys, His, Leu, Phe, Tyr, Trp, and Ile. In contrast, the N-terminal Asn, Gln, Asp, and Glu residues (as well as Cys under some metabolic conditions) are destabilizing owing to their preliminary enzymatic modifications. These modifications include the Nt-deamidation of N-terminal Asn and Gln by the Ntan1 and Ntaq1 Nt-amidases, respectively, and the Nt-arginylation of N-terminal Asp and Glu by the Ate1 arginyltransferase (R-transferase), which can also Nt-arginylate oxidized Cys, either Cys-sulfinate or Cys-sulfonate. These derivatives of N-terminal Cys can form through oxidation of Cys by NO and oxygen, as has been shown by studies with Cys-based physiological N-end rule substrates in animal and plant cells. In addition to its type 1 and type 2 binding sites that recognize, respectively, the basic and bulky hydrophobic destabilizing N-terminal residues, an N-recognin such as Ubr1 contains other substrate-binding sites as well. These sites recognize substrates that are targeted through their internal (non–N-terminal) degrons, as indicated on the diagram (1). Hemin (Fe^{3+}-heme) binds to the Ate1 R-transferase, inhibits its Nt-arginylation activity, and accelerates its in vivo degradation. Hemin also binds to Ubr1 (and apparently to other N-recognins as well) and alters its functional properties, in ways that remain to be understood (13). It was recently shown that both yeast and mammalian Ubr1 can recognize not only the unacetylated primary destabilizing N-terminal residues cited above, but also the unacetylated N-terminal Met residue, if it is followed by a hydrophobic residue. This capability of the Arg/N-end rule pathway greatly expands the range of its substrates, as virtually all nascent proteins bear N-terminal Met (59). This aspect of the Arg/N-end rule pathway is not depicted in the diagram, as it has been characterized thus far only in *Saccharomyces cerevisiae* (59).

Part B. The Ac/N-end rule pathway: The diagram illustrates the mammalian Ac/N-end rule pathway through extrapolation from its *S. cerevisiae* version. [Although it is virtually certain that this pathway is present in all eukaryotes (1), it has been characterized thus far only in *S. cerevisiae* (59–61)]. Red arrow on the left indicates the removal of N-terminal Met by Met-aminopeptidases (MetAPs). N-terminal Met is retained if a residue at position 2 is nonpermissive (too large) for MetAPs. If the retained N-terminal Met or N-terminal Ala, Ser, and Thr are followed by acetylation-permissive residues, the above N-terminal residues are Nt-acetylated by ribosome-associated Nt-acetylases (62–64). Nt-terminal Val and Cys are Nt-acetylated relatively rarely, whereas N-terminal Pro and Gly are almost never Nt-acetylated. N-degrons of the Ac/N-end rule pathway are called Ac/N-degrons to distinguish them from other N-degrons (1). The term secondary refers to the Nt-acetylation of a destabilizing N-terminal residue before a protein can be recognized by a cognate N-recognin. Natural Ac/N-degrons are regulated by their reversible steric shielding in protein complexes (59, 60).

Detailed (Extended) Legend to Fig. 2. Calpain-generated C-terminal fragments of mammalian proteins that are either identified or predicted substrates of the Arg/N-end rule pathway.

The entries whose numbers are colored in green are the experimentally identified (most of them in the present study) substrates of the Arg/N-end rule pathway. The entries whose numbers are colored in black are predicted Arg/N-end rule substrates. Each entry cites a calpain-generated C-terminal (Ct) fragment of a protein and the fragment's N-terminal residue (in red, using three-letter abbreviations for amino acids), followed by a description of uncleaved (full-length) precursor protein. A calpain cleavage site, denoted by an arrowhead, uses single-letter abbreviations for amino acids. An enlarged P1′ residue (in red) becomes N-terminal upon the cleavage. The indicated residue numbers are the number of the first shown residue of a full-length protein and the number of its last residue, respectively. All entries are mouse proteins, with the exception of #14 and #27, which are human proteins. #1: *Glu*-Bak is the proapoptotic Ct fragment of the apoptotic regulator BAK. Glu-BAK is generated by calpain-1 in vitro and is apparently formed in vivo as well (65) (Figs. 3*A* and 5 *E* and *F*). #2: *Arg*-Bid. Bid is a 22-kDa member of the BCL-2 family of apoptosis regulators (66–68). Although full-length Bid is a proapoptotic factor, its C-terminal fragments, which can be naturally produced by activated caspases, calpains or granzyme B, can be even more active than intact Bid as proapoptotic proteins (69). The cleavage of Bid by calpains produces the 14-kDa *Arg*71-Bid fragment (69–72) that has been shown by us to be a short-lived substrate of the Arg/N-end rule pathway (23). #3: *Asp*-Bcl_{XL}. Bcl_{XL} is a 26-kDa antiapoptotic regulatory protein (66, 73). Under conditions that include glucose and oxygen deprivation, Bcl_{XL} can be cleaved by activated calpain-1, resulting in the 21-kDa Asp61-Bcl_{XL} fragment. In contrast to full-length Bcl_{XL}, the *Asp*61-Bcl_{XL} fragment has proapoptotic activity (74) and has been shown by us to be a short-lived substrate of the Arg/N-end rule pathway (23). #4: *Arg*-c-Fos is the Ct fragment of the c-Fos transcriptional regulator. c-Fos is targeted for conditional degradation through more than one degron, including the path that includes the cleavage by calpains (75) (Fig. S1*A* and Fig. 5 *K* and *L*). #5: *Glu*-IκBα is the Ct fragment of the IκBα subunit of the NFκB-IκBα complex in which the NFκB transcriptional

regulator is inhibited by IκBα. The IκBα subunit is targeted for degradation either through a conditional phosphodegron or through a specific calpain-mediated cleavage (76) (Figs. 3*C* and 5 *I* and *J*). #6: *Arg*-Igfbp2 is the calpain-generated Ct fragment of the insulin-like growth factor binding protein-2 (77) (Fig. S1*C* and Fig. 5 *G* and *H*). #7: *Asp*-Capns1 is the Ct fragment of the calpain regulatory subunit that is cleaved by activated calpains (78, 79) (Figs. 3*F* and 5 *A* and *B*). #8: *Arg*-Atp2b2 is the Ct fragment of the transmembrane Atp2b2 plasma membrane Ca^{2+} pump (PMCA) that ejects Ca^{2+} from cells. This pump is activated either by the binding of Ca^{2+}/calmodulin or by the calpain-mediated truncation of Atp2b2 that generates the *Lys*-Atp2b2 fragment and thereby activates the pump (80) (Fig. S1*E* and Fig. 4 *J* and *K*). #9: *Leu*-Capn1 is the natural autogenerated, catalytically active Ct fragment of calpain-1 (81, 82) (Fig. S1*B* and Fig. 5 *C* and *D*). #10: *Arg*-Ankrd2. Ankrd2 (Marp2, Arpp), a member of the MARP (muscle ankyrin repeat protein) family, functions as a negative regulator of muscle differentiation (83). Calpains can produce the 30-kDa *Arg*103-Ankrd2 fragment (84) (Figs. 3*E* and 4 *F* and *G*). #11: *Tyr*-Grm1. Grm1 is the Ct fragment of the mGluR1α transmembrane metabotropic glutamate receptor (85). Receptors containing the calpain-truncated mGluR1α subunit could elevate cytosolic Ca^{2+} but could not activate PI_3K-Akt signaling pathways, in contrast to uncleaved receptors (85, 86) (Figs. 3*B* and 4 *H* and *I*). #12: *Lys*-Ica512. Ica512 (Ptprn) is a member of the transmembrane receptor protein phosphatase family (87). The 43-kDa calpain-generated mouse *Lys*609-Ica512 fragment enters the nucleus and acts as a transcriptional regulator (87, 88) (Fig. S1*D* and Fig. 4 *D* and *E*). #13: *Phe*-GluN2a. GluN2a (NMDA-R2a) is a subunit of the NMDA receptor (NMDAR), a glutamate receptor that can function as a ligand-gated Ca^{2+} channel (89, 90). The GluN2b subunit of NMDAR can also be cleaved by calpains (91). Ct fragments of NR2A and NR2B contain domains required for the association of these subunits with other synaptic proteins. NMDAR receptors lacking the Ct region of GluN2a could function as glutamate-gated Ca^{2+} channels but the intracellular traffic of cleaved receptors, and their electrophysiological properties were altered (92) (Figs. 3*D* and 4 *B* and *C*). #14: *Asn*-DSCR1 (Rcan1) is the calpain-generated Ct fragment of the Down syndrome critical region 1 protein Dscr1, which binds to Raf1, inhibits the phosphatase activity of calcineurin, and enhances its degradation. The *Asn*-DSCR1 fragment does not bind to the Raf1 kinase (93). #15: *Arg*-Glyt1a is the Ct fragment of the transmembrane Glyt1a glycine transporter (94). Another Gly transporter, Glyt1b, is also cleaved by calpains, yielding the *Arg*-Glyt1b fragment (94). These Ct fragments are still active as transporters but are impaired in their ability to remove Gly (an inhibitory neurotransmitter) from synaptic clefts (94). #16: *Asn*-$Ca_v1.1$ is the Ct fragment of the voltage-gated transmembrane Ca^{2+} channel. This (apparently) calpain-generated fragment is noncovalently associated with the rest of the channel and can inhibit its activity. Upon dissociation from the channel, the *Asn*-$Ca_v1.1$ fragment enters the nucleus and functions as a transcriptional regulator (95–98). #17: *Lys*-cortactin is the Ct fragment of cortactin, an actin-binding protein that regulates actin polymerization (99). #18: *Asn*-Bfl-1. Bfl-1 is antiapoptotic regulatory protein whose cleavage by calpain-1 generates the *Asn*72-Bfl-1 Ct proapoptotic fragment (100). #19: *Arg*-dystrophin is the calpain-generated Ct fragment of a major cytoskeletal protein in the skeletal muscle (101). #20: *Gln*-Ryr1 is the Ct fragment of the Ryr1 ryanodine receptor, a Ca^{2+} channel in the ER (102) that mediates the efflux of Ca^{2+} from the ER into the cytosol. Calpain-mediated cleavage of Ryr1 increases Ca^{2+} efflux (103). #21: *Arg*-Mef2d is the Ct fragment of the Mef2d myocyte enhancer factor 2d, a transcriptional regulator that contributes to neuronal survival, development, and synaptic plasticity (104). #22: *Gln*-talin is the calpain-generated Ct fragment of talin, an adaptor protein that interacts with the integrin family of cell adhesion transmembrane proteins (80, 105, 106). #23: *Arg*-p39 is the calpain-generated Ct fragment of the p39 activator of the Cdk5 protein kinase (107). The indicated cleavage site is located immediately downstream of two other closely spaced (and strongly conserved) calpain cleavage sites in p39. A cleavage at any one of these sites yields a predicted Arg/N-end rule substrate. #24: *Gln*-Egfr is one of calpain-generated Ct fragments of the transmembrane epidermal growth factor (EGF) receptor protein kinase (108). Remarkably, all seven calpain cleavage sites in the cytosol-exposed domain of the 170-kDa EGFR contain P1′ residues that are destabilizing in the Arg/N-end rule (108). #25: *Leu*-β-catenin is the calpain-generated Ct-fragment of β-catenin, a conditionally short-lived cytoskeletal protein and transcriptional regulator. The *Leu*-β-catenin fragment is a nuclear protein that activates specific genes in conjunction with other transcription factors (109). #26: *Leu*-NF2 is the calpain-generated Ct fragment of NF2 (merlin), a tumor suppressor and cytoskeletal protein. Loss of function NF2 mutants result in autosomal-dominant neurofibromatosis, a predisposition to specific kinds of brain tumors (110). #27: *Arg*-caspase-9 is the Ct fragment of caspase-9, which can be inactivated by calpains (111), followed by the (predicted) degradation of the Arg-caspase-9 fragment by the Arg/N-end rule pathway. #28: *Leu*-troponin T2 is the Ct fragment of the cardiac troponin T that is produced by calpain-1 in the troponin-containing cardiac myofibril complex (112). #29: *Lys*-PKCα is the calpain-generated Ct fragment of PKCα, a broadly expressed Ser/Thr kinase of the PKC family (113). Being catalytically active but no longer controlled by the regulatory Nt domain of the full-length PKCα, the Lys-PKCα fragment can be toxic, for example, upon its formation in an ischemic heart (114). #30: *Leu*-Rad21 is the calpain-generated Ct-fragment of the Scc1/Rad21 subunit of the chromosome-associated cohesin complex (115). The calpain-mediated generation of *Leu*-Rad21 contributes to the control of chromosome cohesion/segregation, together with processes that include the separase-mediated cleavage of the same Rad21 subunit (32, 115–117). #31: *Phe*-PKCγ is the calpain-generated Ct fragment of PKCγ, a Ser/Thr kinase of the PKC family (113). The *Phe*-PKCγ fragment is constitutively active as a kinase, because it lacks the regulatory Nt domain of the full-length PKCγ kinase (113). #32: *Leu*-$STEP_{33}$ is the Ct fragment of the striatal-enriched $STEP_{61}$ phosphatase, a brain-specific Tyr-phosphatase whose substrates include the MAPK-family kinases ERK1/2 and p38. The calpain-generated *Leu*-$STEP_{33}$ fragment lacks phosphatase activity (118). #33: *Leu*-Camk-IV is the calpain-generated Ct fragment of the Ca^{2+}/calmodulin-dependent kinase-IV. This fragment lacks kinase activity (119). #34: *Leu*-vimentin is the calpain-generated Ct fragment of vimentin, a component of intermediate filaments (120).

SI Materials and Methods

Miscellaneous Reagents. Cycloheximide and calcium ionophore A23187 were from Sigma. Calpain inhibitor carbobenzoxy-valinyl-phenylalaninal (zVF) was from Calbiochem. Mouse and human cDNAs encoding proteins examined in the present work were from OpenBiosystems. Anti-flag M2 Magnetic Beads (M8823; Sigma) were used for immunoprecipitation. Immunoblotting was carried out using the anti-flag monoclonal mouse M2 antibody (Sigma), the HRP-conjugated goat anti-mouse antibody (#170–6516; BioRad), and ECL Prime Western Blotting Detection System (GE Healthcare), according to the manufacturers' protocols.

Plasmids, cDNAs, and Primers. Turbo *Escherichia coli* [New England Biolabs (NEB)] was used for cloning and maintaining plasmids. Phusion High-Fidelity DNA polymerase (NEB) was used for PCR. All constructed plasmids were verified by DNA sequencing.

In some Ub reference technique (URT)-based assays, a test protein migrated, upon SDS/PAGE, too close to the standard DHFR-Ub reference moiety (Fig. 4*A*). Therefore, a larger version of the reference moiety was constructed for such cases (Fig. 5 *I*

and *K*), through an extension of DHFR-Ub with an N-terminal region of the *E. coli* β-galactosidase (βgal; residues 25–119). A DNA fragment encoding this region of βgal was amplified using the plasmid pKP55-M (Table S1) as a template and primers 1605 and 1606 (Table S2). The resulting fragment was digested with HindIII and BamHI, and cloned into HindIII/BamHI-cut pKP496, yielding pKP582. It contained a region encoding the N-terminal flag tag and ^{f}βgal-DHFR-Ub^{R48}, followed by the multiple cloning site (MCS) SacII-EcoRI-XhoI-ClaI-EcoRV. The pKP582 plasmid was a precursor of some plasmids encoding specific URT-based protein fusions (Table S1).

GluN2a. The mouse *GluN2a* ORF was amplified from a mouse brain cDNA library using primers 1585 and 1587 for *Phe*1279-GluN2a or 1586 and 1587 for *Val*1279-GluN2a (Table S2). The resulting DNA fragments were cut with SacII and ClaI and cloned into SacII/ClaI-cut pKP496 (Table S1), yielding pKP568 and pKP569, respectively.

Ica512. The mouse *Ica512* ORF was amplified using cDNA from OpenBiosystems (ID: 4987532) and primers 1591, 1593, 1597, and 1598 for the *Lys*611-Ica512 protein fragment or 1592, 1593, 1597, and 1598 for the *Val*611-Ica512 fragment (Table S2). The resulting DNA fragments were cut with SacII and ClaI and cloned into SacII/ClaI-cut pKP496, yielding pKP574 and pKP575, respectively. Full-length mouse Ica512 bearing both N-terminal and C-terminal flag tags and an alternative junctional residue (Val) at the calpain cleavage site (they were termed ^{f}Ica512^{f} and ^{f}Ica512^{f}-K609V, respectively) was produced as follows: the 5′ region of the *Ica512* ORF was amplified from the above mouse cDNA library using primers 1632–1637 for WT ^{f}Ica512^{f}, or primers 1632–1636 and 1638 for the mutant ^{f}Ica512^{f} -K609V full-length protein (Table S2). The resulting DNA fragments were cut with HindIII and AfeI and were cloned into HindIII/AfeI-cut pKP574, yielding pKP599 and pKP600, respectively (Table S1).

Ankrd2. The mouse *Ankrd2* ORF was amplified using cDNA from OpenBiosystems (ID: 8861782) and primers 1570 and 1572 for the *Arg*103-Ankrd2 fragment or 1571 and 1572 for the *Val*103-Ankrd2 fragment. The resulting DNA fragments were cut with SacII and ClaI and cloned into SacII/ClaI-cut pKP496, yielding pKP576 and pKP577, respectively (Table S1).

Grm1. The mouse *Grm1* ORF was amplified using cDNA from OpenBiosystems (ID: 30544252) and primers 1579 and 1581 for the Tyr937-GRM1 fragment or 1580 and 1581 for the *Val*937-GRM1 fragment. The resulting DNA fragments were cut with SacII and ClaI and cloned into SacII/ClaI-cut pKP496, yielding pKP564 and pKP565, respectively (Table S1).

Atp2b2. The mouse *Atp2B2* ORF was amplified from the above mouse cDNA library using primers 757 and 759 for the *Arg*1091-Atp2b2 fragment or 758 and 759 for the *Val*1091-ATP2B2 fragment. The resulting DNA fragments were cut with SacII and EcoRV and cloned into SacII/ EcoRV-cut pKP496, yielding pJO386 and pJO387, respectively (Table S1).

Capns1. The mouse *Capns1* ORF was amplified from the above mouse cDNA library using primers 1576 and 1578 for the *Asp*142-CAPNS1 fragment or 1577 and 1578 for the *Val*142-Capns1 fragment. The resulting DNA fragments were cut with SacII and ClaI and cloned into SacII/ClaI-cut pKP496, yielding pKP578 and pKP579, respectively (Table S1).

Capn1. The human *Capn1* ORF was amplified using cDNA from OpenBiosystems (ID: 5223130) and primers 1510, 1512, 1513, and 1490 for the *Leu*28-Capn1 fragment or 1511, 1512, 1513, and 1490 for the *Val*28-Capn1 fragment. The resulting DNA fragments were cut with SacII and ClaI and cloned into SacII/ClaI-cut pKP496, yielding pKP536 and pKP537, respectively (Table S1).

Bak. The mouse *Bak* ORF was amplified from the above mouse cDNA library using primers 1610 and 1612 for the *Glu*16-Bak fragment or 1611 and 1612 for the *Val*16-Bak fragment. The resulting DNA fragments were cut with SacII and ClaI and cloned into SacII/ClaI-cut pKP496, yielding pKP583 and pKP584, respectively (Table S1).

Igfbp2. The mouse *Igfbp2* ORF was amplified from a mouse cDNA library using primers 1582 and 1584 for the *Arg*181-IgfbP2 fragment or 1583 and 1584 for the *Val*181-IgfbP2 fragment. The resulting DNA fragments were cut with SacII and ClaI and cloned into SacII/ClaI-cut pKP496, yielding pKP566 and pKP567, respectively (Table S1).

IkBα. The mouse *IκBα* ORF was amplified from the above mouse cDNA library using primers 763 and 765 for the *Glu*51-IκBα fragment or 764 and 765 for the *Val*51- IκBα fragment. The resulting DNA fragments were cut with SacII and ClaI and cloned into SacII/ClaI-cut pKP582, yielding pJO427 and pJO428, respectively (Table S1).

c-Fos. The mouse *c-Fos* ORF was amplified using cDNA from OpenBiosystems (ID: 2582234) and primers 760 and 762 for the *Arg*91-c-Fos fragment or 761 and 762 for the *Val*91-cFOS fragment. The resulting DNA fragments were cut with SacII and ClaI and cloned into SacII/ClaI-cut pKP582, yielding pJO425 and pJO426, respectively (Table S1).

In Vitro Transcription-Translation-Degradation Assays. The TNT T7 Coupled Transcription/Translation System, a version of the Promega's rabbit reticulocyte extract preparation in which the main components of the system were supplied separately, was used to carry out transcription-translation-degradation assays (23, 24, 121). Reaction samples were prepared according to the manufacturer's instructions. Nascent proteins in reticulocyte extract were pulse-labeled with [^{35}S]L-methionine (0.55 mCi/mL, 1,000 Ci/mmol, MP Biomedicals) for 10 min at 30 °C, in the total volume of 30 μL. The labeling was quenched by the addition of cycloheximide and unlabeled methionine to the final concentrations of 0.1 mg/mL and 5 mM, respectively. Samples were withdrawn at indicated time points of a chase. The reactions were terminated by the addition of 0.1 mL of TSD buffer (1% SDS, 5 mM DTT, 50 mM Tris·HCl, pH 7.4) and snap-freezing samples in liquid nitrogen. Samples were then heated at 95 °C for 10 min, diluted with 10 volumes of TNN buffer (0.5% Nonidet P-40, 0.25 M NaCl, 5 mM EDTA, 50 mM Tris·HCl, pH 7.4), containing the complete protease-inhibitor mixture (Roche), clarified by centrifugation at 20,000 × *g* for 5 min, and immunoprecipitated using 5 μL of anti-flag M2 Magnetic Beads. The samples were incubated with rocking at 4 °C for 3 h, followed by three washes in TNN buffer, one wash in 10 mM Tris·HCl (pH 8.5), and resuspension in 20 μL of SDS-sample buffer. The resulting samples were heated at 95 °C for 5 min and fractionated by SDS 4–12% PAGE, followed by autoradiography and quantification, using Storm PhosphorImager (Molecular Dynamics) and ImageQuant (GE Healthcare).

In Vivo URT-Based Degradation Assays. Human HEK293T cells were obtained from American Type Culture Collection (ATCC). Cells were grown at 37 °C with 5% (vol/vol) CO_2 in DMEM supplemented with 10% FBS (Gemini Bio-Products) and penicillin/streptomycin (100 units/mL) (HyClone). Cells were transfected at ∼75% confluency with 0.05–0.2 μg plasmid per 35-mm well using Lipofectamine-2000 (Invitrogen) according to the manufacturer's protocol. Transfected cells were labeled 48 h later for 20 min with [^{35}S]L-methionine (0.1 mCi/mL; MP Biomedicals) in DMEM lacking Met and Cys. The labeling was stopped by the addition of cycloheximide (0.1 mg/mL) in complete DMEM (containing 2.5 mM unlabeled Met as well). Samples (0.1 mL) were withdrawn at indicated times of the chase, mixed with 0.1 mL of TSD buffer (1% SDS, 5 mM DTT, 50 mM Tris·HCl, pH 7.4), and the resulting samples were snap-frozen in liquid nitrogen. Samples were then heated at 95 °C for 10 min and diluted with 10 volumes of TNN buffer (see above) containing the complete protease-inhibitor mixture (Roche). Total ^{35}S radioactivity in-

soluble in 10% (vol/vol) CCl_3COOH was then determined, and volumes were adjusted to equalize ^{35}S among different samples. Thus, treated samples were processed for immunoprecipitation by the addition of 5 μL of anti-flag M2 magnetic beads and incubation with rocking at 4 °C for 3 h. Immunoprecipitated proteins were washed three times in TNN buffer and once in 10 mM Tris·HCl (pH 8.5), followed by the resuspension in 20 μL of SDS sample buffer, heating at 95 °C for 10 min, SDS 4–15% PAGE, and autoradiography with quantification, as described above.

In Vitro Assays with ^{f}Ica512^{f} and ^{f}Ica512^{f}-K609V Full-Length Proteins. A diagram of the N-terminal/C-terminal double tagging of a test protein (to make possible the detection of both products of an in vitro or in vivo protein cleavage) is shown in Fig. 6*A* and described in the main text. The TNT T7 Coupled Transcription/Translation System (Promega) was used to carry out transcription-translation-degradation assays as described above. ^{f}Ica512^{f} and ^{f}Ica512^{f}-K609V^{f} (main text and Fig. 6) were labeled with [^{35}S]methionine (0.55 mCi/mL, 1,000 Ci/mmol; MP Biomedicals) for 60 min, in a total volume of 30 μL, followed by buffer exchange using Zeba Spin Desalting Column (Pierce) equilibrated with CC buffer [10% (vol/vol) glycerol, 50 mM NaCl, 0.5 mM DTT, 20 mM Tris·HCl, pH 7.4]. The cleavage of ^{f}Ica512^{f} and ^{f}Ica512^{f}-K609V^{f} was initiated by the addition of $CaCl_2$ (to the final concentration of 2 mM) and purified human calpain-1 [to a final concentration of 8.5 U/mL (70 nM)]. The mixture was incubated at 30 °C for 30 min, and calpain was inhibited by adding z-VF (to the final concentration of 0.1 mM), followed by buffer exchange using Zeba Spin Desalting Column equilibrated with 1 mM Mg-acetate, 60 mM K-acetate, and 10 mM Tris-acetate (pH 8.2). An equal volume of fresh TNT reticulocyte extract was added to the samples, followed by a chase at 30 °C for 30 and 120 min. Samples were withdrawn at indicated time points of the chase and processed for analysis as described above for URT assays.

In Vivo Assays with ^{f}Ica512^{f} and ^{f}Ica512^{f}-K609V Full-Length Proteins. HEK293T cells were used for in vivo analyses of ^{f}Ica512^{f} and ^{f}Ica512^{f}-K609V. To allow the natural processing and intracellular localization of these ER-translocated, transmembrane proteins, the N-terminal flag tag was placed immediately downstream of the signal peptide of Ica512 (main text). A membrane localization of the in vivo–processed ^{f}Ica512^{f} was verified and confirmed by immunoblotting with anti-flag antibody. Briefly, HEK293T cells were transiently transfected with either a vector plasmid or the otherwise identical plasmid (pKP599 and pKP600, respectively) encoding ^{f}Ica512^{f}. Cells were detached from plates 36 h after transfection by pipetting and were collected by centrifugation at 200 × *g* for 5 min. Pelleted cells were washed with 1 mL ice-cold PBS and resuspended in 0.2 mL PBS-EP (1× PBS supplemented with 2 mM EDTA and 1× Complete Protease Inhibitor; Roche), followed by sonication for 1 min and the initial clarification by centrifugation at 200 × *g* for 5 min. The resulting supernatants [clarified extract (CE); Fig. S2*C*) were centrifuged at 20,000 × *g* for 15 min, yielding soluble cytosol (SC) and pellet [membrane (M)] fractions. The latter fraction was washed with 0.25 mL PBS-EP and resuspended in PBS-EP. Samples of CE, SC, and M fractions were mixed with 3× lithium dodecyl sulfate (LDS) sample buffer (Invitrogen), heated at 70 °C for 10 min, and fractionated by SDS/PAGE, followed by immunoblotting with anti-flag antibody, an antibody to GAPDH (a largely cytosolic protein) and visualization using ECL Plus Detection System (GE Healthcare).

For in vivo degradation assays with ^{f}Ica512^{f} and ^{f}Ica512^{f}-K609V that involved the calpain-induced cleavage of these full-length proteins, HEK293T cells were transfected with plasmids expressing either ^{f}Ica512^{f} and ^{f}Ica512^{f}-K609V. Approximately 48 h after transfection, cells were labeled for 60 min with [^{35}S]L-methionine (0.1 mCi/mL; MP Biomedicals) in DMEM lacking Met and Cys. Calpain-mediated cleavage of ^{f}Ica512^{f} and ^{f}Ica512^{f}-K609V was induced by adding DMEM containing the following additional compounds: 50 μM A23184 (Ca^{2+} ionophore), 3 mM $CaCl_2$, 2.5 mM methionine, 2.5 mM cysteine, and 0.1 mg/mL cycloheximide. Cells were incubated at 37 °C for 60 min. The cell-penetrating calpain inhibitor z-VF was then added to the final concentration of 0.1 mM, followed by a chase for 1.5 and 6 h. Cells were harvested by centrifugation, lysed by the addition of 0.1 mL of TSD buffer, and snap-frozen in liquid nitrogen. Samples were then heated at 95 °C for 10 min and diluted with 10 volumes of TNN buffer, followed by immunoprecipitation with anti-flag M2 magnetic beads, SDS/PAGE, autoradiography, and quantification as described above.

1. Varshavsky A (2011) The N-end rule pathway and regulation by proteolysis. *Protein Sci* 20:1298–1345.
2. Eisele F, Wolf DH (2008) Degradation of misfolded protein in the cytoplasm is mediated by the ubiquitin ligase Ubr1. *FEBS Lett* 582(30):4143–4146.
3. Heck JW, Cheung SK, Hampton RY (2010) Cytoplasmic protein quality control degradation mediated by parallel actions of the E3 ubiquitin ligases Ubr1 and San1. *Proc Natl Acad Sci USA* 107(3):1106–1111.
4. Tasaki TS, Sriram SM, Park KS, Kwon YT (2012) The N-end rule pathway. *Annu Rev Biochem* 81:261–289.
5. Graciet E, Wellmer F (2010) The plant N-end rule pathway: Structure and functions. *Trends Plant Sci* 15(8):447–453.
6. Dougan DA, Micevski D, Truscott KN (2012) The N-end rule pathway: From recognition by N-recognins, to destruction by AAA+proteases. *Biochim Biophys Acta* 1823(1):83–91.
7. Mogk A, Schmidt R, Bukau B (2007) The N-end rule pathway for regulated proteolysis: Prokaryotic and eukaryotic strategies. *Trends Cell Biol* 17(4):165–172.
8. Varshavsky A (1996) The N-end rule: Functions, mysteries, uses. *Proc Natl Acad Sci USA* 93(22):12142–12149.
9. Hwang C-S, Shemorry A, Auerbach D, Varshavsky A (2010) The N-end rule pathway is mediated by a complex of the RING-type Ubr1 and HECT-type Ufd4 ubiquitin ligases. *Nat Cell Biol* 12(12):1177–1185.
10. Hwang C-S, Shemorry A, Varshavsky A (2009) Two proteolytic pathways regulate DNA repair by cotargeting the Mgt1 alkylguanine transferase. *Proc Natl Acad Sci USA* 106(7):2142–2147.
11. Hwang C-S, Varshavsky A (2008) Regulation of peptide import through phosphorylation of Ubr1, the ubiquitin ligase of the N-end rule pathway. *Proc Natl Acad Sci USA* 105(49): 19188–19193.
12. Xia Z, et al. (2008) Substrate-binding sites of UBR1, the ubiquitin ligase of the N-end rule pathway. *J Biol Chem* 283(35):24011–24028.
13. Hu R-G, Wang H, Xia Z, Varshavsky A (2008) The N-end rule pathway is a sensor of heme. *Proc Natl Acad Sci USA* 105(1):76–81.
14. Hu R-G, et al. (2005) The N-end rule pathway as a nitric oxide sensor controlling the levels of multiple regulators. *Nature* 437(7061):981–986.
15. Hwang C-S, et al. (2011) Ubiquitin ligases of the N-end rule pathway: Assessment of mutations in UBR1 that cause the Johanson-Blizzard syndrome. *PLoS ONE* 6(9):e24925.
16. Wang H, Piatkov KI, Brower CS, Varshavsky A (2009) Glutamine-specific N-terminal amidase, a component of the N-end rule pathway. *Mol Cell* 34(6):686–695.
17. Brower CS, Varshavsky A (2009) Ablation of arginylation in the mouse N-end rule pathway: Loss of fat, higher metabolic rate, damaged spermatogenesis, and neurological perturbations. *PLoS ONE* 4(11):e7757.
18. Zenker M, et al. (2005) Deficiency of UBR1, a ubiquitin ligase of the N-end rule pathway, causes pancreatic dysfunction, malformations and mental retardation (Johanson-Blizzard syndrome). *Nat Genet* 37(12):1345–1350.
19. Prasad R, Kawaguchi S, Ng DTW (2010) A nucleus-based quality control mechanism for cytosolic proteins. *Mol Biol Cell* 21(13):2117–2127.
20. Kurosaka S, et al. (2010) Arginylation-dependent neural crest cell migration is essential for mouse development. *PLoS Genet* 6(3):e1000878.
21. Zhang F, Saha S, Shabalina SA, Kashina A (2010) Differential arginylation of actin isoforms is regulated by coding sequence-dependent degradation. *Science* 329(5998):1534–1537.
22. Lee MJ, et al. (2005) RGS4 and RGS5 are in vivo substrates of the N-end rule pathway. *Proc Natl Acad Sci USA* 102(42):15030–15035.
23. Piatkov KI, Brower CS, Varshavsky A (2012) The N-end rule pathway counteracts cell death by destroying proapoptotic protein fragments. *Proc Natl Acad Sci USA* 109(27):E1839–E1847.
24. Piatkov KI, Colnaghi L, Békés M, Varshavsky A, Huang TT (2012) The auto-generated fragment of the Usp1 deubiquitylase is a physiological substrate of the N-end rule pathway. *Mol Cell* 48(6):926–933.
25. Kwon YT, et al. (2002) An essential role of N-terminal arginylation in cardiovascular development. *Science* 297(5578):96–99.
26. Lee MJ, et al. (2012) Characterization of arginylation branch of N-end rule pathway in G-protein-mediated proliferation and signaling of cardiomyocytes. *J Biol Chem* 287(28):24043–24052.
27. Choi WS, et al. (2010) Structural basis for the recognition of N-end rule substrates by the UBR box of ubiquitin ligases. *Nat Struct Mol Biol* 17(10):1175–1181.

28. Matta-Camacho E, Kozlov G, Li FF, Gehring K (2010) Structural basis of substrate recognition and specificity in the N-end rule pathway. *Nat Struct Mol Biol* 17(10): 1182–1187.
29. Licausi F, et al. (2011) Oxygen sensing in plants is mediated by an N-end rule pathway for protein destabilization. *Nature* 479(7373):419–422.
30. Sasidharan R, Mustroph A (2011) Plant oxygen sensing is mediated by the N-end rule pathway: A milestone in plant anaerobiosis. *Plant Cell* 23(12):4173–4183.
31. Gibbs DJ, et al. (2011) Homeostatic response to hypoxia is regulated by the N-end rule pathway in plants. *Nature* 479(7373):415–418.
32. Rao H, Uhlmann F, Nasmyth K, Varshavsky A (2001) Degradation of a cohesin subunit by the N-end rule pathway is essential for chromosome stability. *Nature* 410(6831): 955–959.
33. Kim ST, et al. (2013) The N-end rule proteolytic system in autophagy. *Autophagy* 9(7):1100–1103.
34. Zhang G, Lin RK, Kwon YT, Li YP (2013) Signaling mechanism of tumor cell-induced up-regulation of E3 ubiquitin ligase UBR2. *FASEB J* 27(7):2893–2901.
35. Tasaki T, et al. (2013) UBR box N-recognin-4 (UBR4), an N-recognin of the N-end rule pathway, and its role in yolk sac vascular development and autophagy. *Proc Natl Acad Sci USA* 110(10):3800–3805.
36. Fujiwara H, Tanaka N, Yamashita I, Kitamura K (2013) Essential role of Ubr11, but not Ubr1, as an N-end rule ubiquitin ligase in Schizosaccharomyces pombe. *Yeast* 30(1):1–11.
37. Kitamura K, Fujiwara H (2013) The type-2 N-end rule peptide recognition activity of Ubr11 ubiquitin ligase is required for the expression of peptide transporters. *FEBS Lett* 587(2):214–219.
38. An JY, et al. (2010) UBR2 mediates transcriptional silencing during spermatogenesis via histone ubiquitination. *Proc Natl Acad Sci USA* 107(5):1912–1917.
39. An JY, et al. (2012) UBR2 of the N-end rule pathway is required for chromosome stability via histone ubiquitylation in spermatocytes and somatic cells. *PLoS ONE* 7(5):e37414.
40. Sultana R, Theodoraki MA, Caplan AJ (2012) UBR1 promotes protein kinase quality control and sensitizes cells to Hsp90 inhibition. *Exp Cell Res* 318(1):53–60.
41. Lee P, Sowa ME, Gygi SP, Harper JW (2011) Alternative ubiquitin activation/conjugation cascades interact with N-end rule ubiquitin ligases to control degradation of RGS proteins. *Mol Cell* 43(3):392–405.
42. Román-Hernández G, Hou JY, Grant RA, Sauer RT, Baker TA (2011) The ClpS adaptor mediates staged delivery of N-end rule substrates to the AAA+ ClpAP protease. *Mol Cell* 43(2):217–228.
43. Yang F, et al. (2010) The ubiquitin ligase Ubr2, a recognition E3 component of the N-end rule pathway, stabilizes Tex19.1 during spermatogenesis. *PLoS ONE* 5(11): e14017.
44. Ninnis RL, Spall SK, Talbo GH, Truscott KN, Dougan DA (2009) Modification of PATase by L/F-transferase generates a ClpS-dependent N-end rule substrate in Escherichia coli. *EMBO J* 28(12):1732–1744.
45. Schmidt R, Zahn R, Bukau B, Mogk A (2009) ClpS is the recognition component for Escherichia coli substrates of the N-end rule degradation pathway. *Mol Microbiol* 72(2):506–517.
46. Holman TJ, et al. (2009) The N-end rule pathway promotes seed germination and establishment through removal of ABA sensitivity in Arabidopsis. *Proc Natl Acad Sci USA* 106(11):4549–4554.
47. Cai H, Hauser M, Naider F, Becker JM (2007) Differential regulation and substrate preferences in two peptide transporters of Saccharomyces cerevisiae. *Eukaryot Cell* 6(10):1805–1813.
48. Schnupf P, Zhou J, Varshavsky A, Portnoy DA (2007) Listeriolysin O secreted by *Listeria monocytogenes* into the host cell cytosol is degraded by the N-end rule pathway. *Infect Immun* 75(11):5135–5147.
49. Hu R-G, et al. (2006) Arginyltransferase, its specificity, putative substrates, bidirectional promoter, and splicing-derived isoforms. *J Biol Chem* 281(43):32559–32573.
50. Graciet E, et al. (2006) Aminoacyl-transferases and the N-end rule pathway of prokaryotic/eukaryotic specificity in a human pathogen. *Proc Natl Acad Sci USA* 103(9):3078–3083.
51. Kurosaka S, et al. (2012) Arginylation regulates myofibrils to maintain heart function and prevent dilated cardiomyopathy. *J Mol Cell Cardiol* 53(3):333–341.
52. Wang J, et al. (2011) Arginyltransferase is an ATP-independent self-regulating enzyme that forms distinct functional complexes in vivo. *Chem Biol* 18(1):121–130.
53. Decca MB, et al. (2007) Post-translational arginylation of calreticulin: A new isospecies of calreticulin component of stress granules. *J Biol Chem* 282(11): 8237–8245.
54. Tobias JW, Shrader TE, Rocap G, Varshavsky A (1991) The N-end rule in bacteria. *Science* 254(5036):1374–1377.
55. Boso G, Tasaki T, Kwon YT, Somia NV (2013) The N-end rule and retroviral infection: No effect on integrase. *Virol J* 10:233.
56. Saha S, Kashina A (2011) Posttranslational arginylation as a global biological regulator. *Dev Biol* 358(1):1–8.
57. Belzil C, et al. (2013) A Ca2+-dependent mechanism of neuronal survival mediated by the microtubule-associated protein p600. *J Biol Chem* 288(34):24452–24464.
58. Yamano K, Youle RJ (2013) PINK1 is degraded through the N-end rule pathway. *Autophagy* 9(11):1758–1769.
59. Kim H-K, et al. (2014) The N-terminal methionine of cellular proteins as a degradation signal. *Cell* 156(1-2):158–169.
60. Shemorry A, Hwang C-S, Varshavsky A (2013) Control of protein quality and stoichiometries by N-terminal acetylation and the N-end rule pathway. *Mol Cell* 50(4):540–551.
61. Hwang C-S, Shemorry A, Varshavsky A (2010) N-terminal acetylation of cellular proteins creates specific degradation signals. *Science* 327(5968):973–977.
62. Arnesen T, et al. (2009) Proteomics analyses reveal the evolutionary conservation and divergence of N-terminal acetyltransferases from yeast and humans. *Proc Natl Acad Sci USA* 106(20):8157–8162.
63. Starheim KK, Gevaert K, Arnesen T (2012) Protein N-terminal acetyltransferases: When the start matters. *Trends Biochem Sci* 37(4):152–161.
64. Van Damme P, et al. (2012) N-terminal acetylome analyses and functional insights of the N-terminal acetyltransferase NatB. *Proc Natl Acad Sci USA* 109(31):12449–12454.
65. Moldoveanu T, et al. (2006) The X-ray structure of a BAK homodimer reveals an inhibitory zinc binding site. *Mol Cell* 24(5):677–688.
66. Green DR (2011) *Means to an End: Apoptosis and Other Cell Death Mechanisms* (Cold Spring Harbor Laboratory Press, Cold Spring Harbor, NY).
67. Yin X-M (2006) Bid, a BH3-only multifunctional molecule, is at the cross road of life and death. *Gene* 369:7–19.
68. Billen LP, Shamas-Din A, Andrews DW (2008) Bid: A Bax-like BH3 protein. *Oncogene* 27(Suppl 1):S93–S104.
69. Chen M, et al. (2001) Bid is cleaved by calpain to an active fragment in vitro and during myocardial ischemia/reperfusion. *J Biol Chem* 276(33):30724–30728.
70. Mandic A, et al. (2002) Calpain-mediated Bid cleavage and calpain-independent Bak modulation: Two separate pathways in cisplatin-induced apoptosis. *Mol Cell Biol* 22(9):3003–3013.
71. Gil-Parrado S, et al. (2002) Ionomycin-activated calpain triggers apoptosis. A probable role for Bcl-2 family members. *J Biol Chem* 277(30):27217–27226.
72. Cabon L, et al. (2012) BID regulates AIF-mediated caspase-independent necroptosis by promoting BAX activation. *Cell Death Differ* 19(2):245–256.
73. García-Sáez AJ, Ries J, Orzáez M, Pérez-Payà E, Schwille P (2009) Membrane promotes tBID interaction with BCL(XL). *Nat Struct Mol Biol* 16(11):1178–1185.
74. Nakagawa T, Yuan J (2000) Cross-talk between two cysteine protease families. Activation of caspase-12 by calpain in apoptosis. *J Cell Biol* 150(4):887–894.
75. Pariat M, et al. (2000) The sensitivity of c-Jun and c-Fos proteins to calpains depends on conformational determinants of the monomers and not on formation of dimers. *Biochem J* 345(Pt 1):129–138.
76. Schaecher K, Goust JM, Banik NL (2004) The effects of calpain inhibition on IkB alpha degradation after activation of PBMCs: Identification of the calpain cleavage sites. *Neurochem Res* 29(7):1443–1451.
77. Berg U, Bang P, Carlsson-Skwirut C (2007) Calpain proteolysis of insulin-like growth factor binding protein (IGFBP) -2 and -3, but not of IGFBP-1. *Biol Chem* 388(8): 859–863.
78. Ono Y, Sorimachi H (2012) Calpains: An elaborate proteolytic system. *Biochim Biophys Acta* 1824(1):224–236.
79. Goll DE, Thompson VF, Li H, Wei W, Cong J (2003) The calpain system. *Physiol Rev* 83(3):731–801.
80. Di Leva F, Domi T, Fedrizzi L, Lim D, Carafoli E (2008) The plasma membrane Ca2+ ATPase of animal cells: Structure, function and regulation. *Arch Biochem Biophys* 476(1):65–74.
81. Brown N, Crawford C (1993) Structural modifications associated with the change in Ca2+ sensitivity on activation of m-calpain. *FEBS Lett* 322(1):65–68.
82. Molinari M, Anagli J, Carafoli E (1994) Ca(2+)-activated neutral protease is active in the erythrocyte membrane in its nonautolyzed 80-kDa form. *J Biol Chem* 269(45): 27992–27995.
83. Bean C, Facchinello N, Faulkner G, Lanfranchi G (2008) The effects of Ankrd2 alteration indicate its involvement in cell cycle regulation during muscle differentiation. *Biochim Biophys Acta* 1783(6):1023–1035.
84. Hayashi C, et al. (2008) Multiple molecular interactions implicate the connectin/titin N2A region as a modulating scaffold for p94/calpain 3 activity in skeletal muscle. *J Biol Chem* 283(21):14801–14814.
85. Xu W, et al. (2007) Calpain-mediated mGluR1alpha truncation: A key step in excitotoxicity. *Neuron* 53(3):399–412.
86. Niswender CM, Conn PJ (2010) Metabotropic glutamate receptors: Physiology, pharmacology, and disease. *Annu Rev Pharmacol Toxicol* 50:295–322.
87. Trajkovski M, et al. (2004) Nuclear translocation of an ICA512 cytosolic fragment couples granule exocytosis and insulin expression in beta-cells. *J Cell Biol* 167(6): 1063–1074.
88. Ort T, et al. (2001) Dephosphorylation of beta2-syntrophin and Ca2+/mu-calpain-mediated cleavage of ICA512 upon stimulation of insulin secretion. *EMBO J* 20(15): 4013–4023.
89. Bi R, Rong Y, Bernard A, Khrestchatisky M, Baudry M (2000) Src-mediated tyrosine phosphorylation of NR2 subunits of N-methyl-D-aspartate receptors protects from calpain-mediated truncation of their C-terminal domains. *J Biol Chem* 275(34): 26477–26483.
90. Collingridge GL, Olsen RW, Peters J, Spedding M (2009) A nomenclature for ligand-gated ion channels. *Neuropharmacology* 56(1):2–5.
91. Simpkins KL, et al. (2003) Selective activation induced cleavage of the NR2B subunit by calpain. *J Neurosci* 23(36):11322–11331.
92. Steigerwald F, et al. (2000) C-Terminal truncation of NR2A subunits impairs synaptic but not extrasynaptic localization of NMDA receptors. *J Neurosci* 20(12):4573–4581.
93. Cho Y-J, Abe M, Kim SY, Sato Y (2005) Raf-1 is a binding partner of DSCR1. *Arch Biochem Biophys* 439(1):121–128.
94. Baliova M, Jursky F (2005) Calpain sensitive regions in the N-terminal cytoplasmic domains of glycine transporters GlyT1A and GlyT1B. *Neurochem Res* 30(9): 1093–1100.
95. Catterall WA (2011) Voltage-gated calcium channels. *Cold Spring Harb Perspect Biol* 3(8):a003947.
96. Hulme JT, et al. (2005) Sites of proteolytic processing and noncovalent association of the distal C-terminal domain of CaV1.1 channels in skeletal muscle. *Proc Natl Acad Sci USA* 102(14):5274–5279.

97. Hulme JT, Yarov-Yarovoy V, Lin TWC, Scheuer T, Catterall WA (2006) Autoinhibitory control of the CaV1.2 channel by its proteolytically processed distal C-terminal domain. *J Physiol* 576(Pt 1):87–102.
98. Gomez-Ospina N, Tsuruta F, Barreto-Chang O, Hu L, Dolmetsch R (2006) The C terminus of the L-type voltage-gated calcium channel Ca(V)1.2 encodes a transcription factor. *Cell* 127(3):591–606.
99. Perrin BJ, Amann KJ, Huttenlocher A (2006) Proteolysis of cortactin by calpain regulates membrane protrusion during cell migration. *Mol Biol Cell* 17(1):239–250.
100. Valero JG, et al. (2012) μ-Calpain conversion of antiapoptotic Bfl-1 (BCL2A1) into a prodeath factor reveals two distinct alpha-helices inducing mitochondria-mediated apoptosis. *PLoS ONE* 7(6):e38620.
101. Yoshida M, Suzuki A, Shimizu T, Ozawa E (1992) Proteinase-sensitive sites on isolated rabbit dystrophin. *J Biochem* 112(4):433–439.
102. Wu Y, et al. (1997) Functional interactions between cytoplasmic domains of the skeletal muscle Ca2+ release channel. *J Biol Chem* 272(40):25051–25061.
103. Shoshan-Barmatz V, Weil S, Meyer H, Varsanyi M, Heilmeyer LM (1994) Endogenous, Ca(2+)-dependent cysteine-protease cleaves specifically the ryanodine receptor/Ca2+ release channel in skeletal muscle. *J Membr Biol* 142(3):281–288.
104. Wei G, et al. (2012) Calpain-mediated degradation of myocyte enhancer factor 2D contributes to excitotoxicity by activation of extrasynaptic N-methyl-D-aspartate receptors. *J Biol Chem* 287(8):5797–5805.
105. Rees DJG, Ades SE, Singer SJ, Hynes RO (1990) Sequence and domain structure of talin. *Nature* 347(6294):685–689.
106. Bate N, et al. (2012) Talin contains a C-terminal calpain2 cleavage site important in focal adhesion dynamics. *PLoS ONE* 7(4):e34461.
107. Patzke H, Tsai LH (2002) Calpain-mediated cleavage of the cyclin-dependent kinase-5 activator p39 to p29. *J Biol Chem* 277(10):8054–8060.
108. Gregoriou M, Willis AC, Pearson MA, Crawford C (1994) The calpain cleavage sites in the epidermal growth factor receptor kinase domain. *Eur J Biochem* 223(2):455–464.
109. Abe K, Takeichi M (2007) NMDA-receptor activation induces calpain-mediated beta-catenin cleavages for triggering gene expression. *Neuron* 53(3):387–397.
110. Kimura Y, et al. (1998) The involvement of calpain-dependent proteolysis of the tumor suppressor NF2 (merlin) in schwannomas and meningiomas. *Nat Med* 4(8): 915–922.
111. Chua BT, Guo K, Li P (2000) Direct cleavage by the calcium-activated protease calpain can lead to inactivation of caspases. *J Biol Chem* 275(7):5131–5135.
112. Zhang Z, Biesiadecki BJ, Jin JP (2006) Selective deletion of the NH2-terminal variable region of cardiac troponin T in ischemia reperfusion by myofibril-associated mu-calpain cleavage. *Biochemistry* 45(38):11681–11694.
113. Kishimoto A, et al. (1989) Limited proteolysis of protein kinase C subspecies by calcium-dependent neutral protease (calpain). *J Biol Chem* 264(7):4088–4092.
114. Kang MY, et al. (2010) Receptor-independent cardiac protein kinase Calpha activation by calpain-mediated truncation of regulatory domains. *Circ Res* 107(7): 903–912.
115. Panigrahi AK, Zhang N, Mao Q, Pati D (2011) Calpain-1 cleaves Rad21 to promote sister chromatid separation. *Mol Cell Biol* 31(21):4335–4347.
116. Hauf S, Waizenegger IC, Peters J-M (2001) Cohesin cleavage by separase required for anaphase and cytokinesis in human cells. *Science* 293(5533):1320–1323.
117. Varshavsky A (2008) Discovery of cellular regulation by protein degradation. *J Biol Chem* 283(50):34469–34489.
118. Xu J, et al. (2009) Extrasynaptic NMDA receptors couple preferentially to excitotoxicity via calpain-mediated cleavage of STEP. *J Neurosci* 29(29):9330–9343.
119. McGinnis KM, Whitton MM, Gnegy ME, Wang KK (1998) Calcium/calmodulin-dependent protein kinase IV is cleaved by caspase-3 and calpain in SH-SY5Y human neuroblastoma cells undergoing apoptosis. *J Biol Chem* 273(32):19993–20000.
120. Fischer S, Vandekerckhove J, Ampe C, Traub P, Weber K (1986) Protein-chemical identification of the major cleavage sites of the Ca2+ proteinase on murine vimentin, the mesenchymal intermediate filament protein. *Biol Chem Hoppe Seyler* 367(11):1147–1152.
121. Brower CS, Piatkov KI, Varshavsky A (2013) Neurodegeneration-associated protein fragments as short-lived substrates of the N-end rule pathway. *Mol Cell* 50(2):161–171.

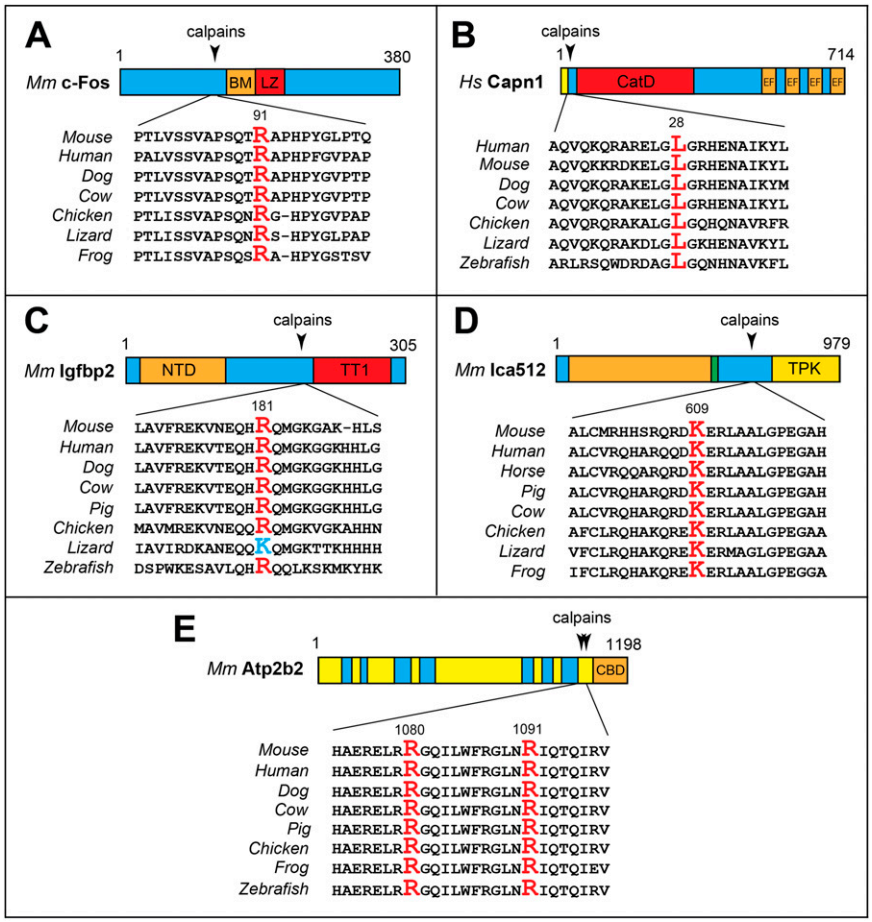

Fig. S1. Evolutionary conservation of destabilizing activity of P1′ residues in calpain cleavage sites. Arrowheads indicate calpain cleavage sites. P1′ residues, which become N-terminal upon the cleavage, are larger and colored. Domain organization and approximate location of a calpain cleavage site are indicated for each protein. Specific positions of P1′ residues are indicated as well for the first cited protein in a sequence alignment, specifically, for the human [*Homo sapiens* (*Hs*)] calpain-1 (Capn1) in *B* and for the mouse [*Mus musculus* (*Mm*)] proteins in *A* and *C*–*E*. See the main text for descriptions of the cited proteins. (*A*) c-Fos. (*B*) Capn1. (*C*) Igfbp2. (*D*) Ica512. (*E*) Atp2b2.

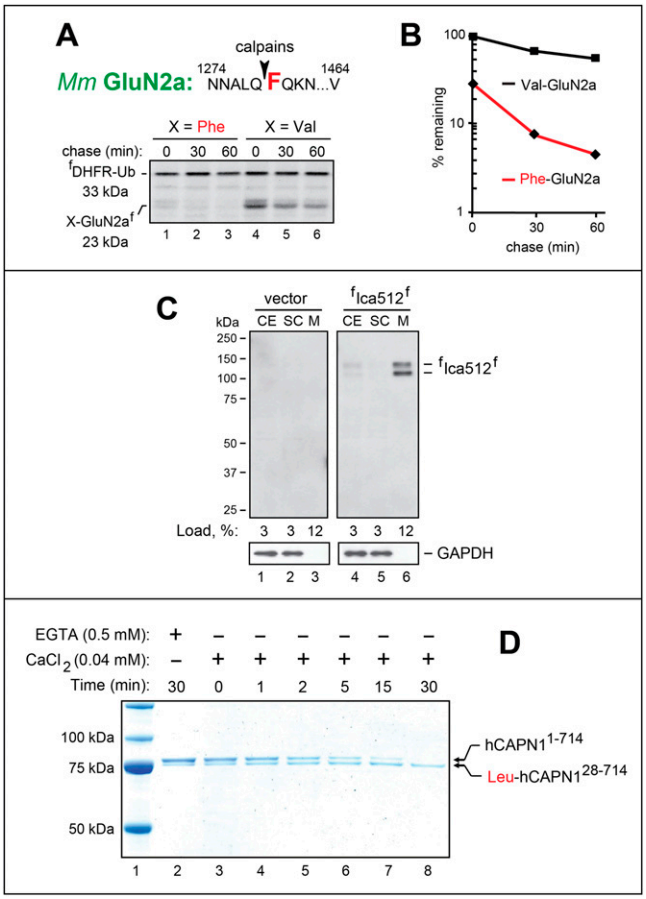

Fig. S2. In vivo degradation of a calpain-generated protein fragment. (*A*) HEK293T cells were transiently transfected with URT-based plasmids (Fig. 4*A*) expressing the Phe1279-GluN2a^{f} fragment (Figs. 2, #13, 3*D*, and 4*B*) or the otherwise identical Val1279-GluN2a^{f} fragment. Cells were labeled for 20 min with [^{35}S]methionine, followed by a chase for 30 and 60 min, immunoprecipitation of cell extracts with anti-flag antibody, SDS/PAGE, and autoradiography (*SI Materials and Methods*). (*B*) Quantification of data in *A*. (*C*) Verification of the predominantly membrane localization of ^{f}lca512^{f} in vivo. HEK293T cells were transiently transfected either with a plasmid expressing doubly flag-tagged, full-length ^{f}lca512^{f} (Fig. 6*A*) or with vector alone. Cell extracts were clarified by a brief low-speed centrifugation (200 × *g* for 5 min; *SI Materials and Methods*). The supernatants [clarified extract (CE)] were centrifuged at 20,000 × *g* for 15 min to pellet cell membranes, yielding the membrane (M) and soluble cytosol (SC) fractions. The resulting samples were subjected to SDS/PAGE, followed by immunoblotting with anti-flag antibody and antibody to GAPDH, a largely cytosolic protein. The notation "load, %" indicates relative amounts of fractions subjected to SDS/PAGE. Lanes 1–3, immunoblotting analyses of CE, SC, and M fractions from HEK293T cells transfected with vector alone. Lanes 4–6, same as lanes 1–3 but cells were transfected with the plasmid expressing ^{f}lca512^{f}. (*D*) Autoprocessing of calpain. Purified human calpain-1 (*SI Materials and Methods*) in 10% (vol/vol) glycerol, 50 mM NaCl, 0.5 mM DTT, and 20 mM Tris·HCl (pH 7.4) was shifted to 40 μM $CaCl_2$ in the same buffer, followed by SDS/PAGE and Coomassie staining at indicated time points. Lane 1, molecular mass markers. Lane 2, a 30-min incubation of calpain-1 under the above conditions plus 0.5 mM EGTA, a Ca^{2+}-chelating compound. Lanes 3–8, same as lane 2 but no EGTA and incubation times from 0 to 30 min, as indicated.

Table S1. Plasmids used in this study

Plasmid	Description	Source or reference
pcDNA3.0-Neo	Amp^R; Neo^R; Expression vector for cloning your gene of interest	Invitrogen
Clone: 8861782	Amp^R; fragment of mouse Ankrd2 cDNA	Open Biosystems
Clone: 5223130	Amp^R; full length human Capn1 cDNA	Open Biosystems
Clone: 5749709	Amp^R; full length human Capn2 cDNA	Open Biosystems
Clone: 30544252	Amp^R; full length mouse Grm1 cDNA	Open Biosystems
Clone: 4987532	Amp^R; fragment of mouse Ica512 cDNA	Open Biosystems
Clone: 2582234	Amp^R; full length mouse c-Fos cDNA	Open Biosystems
pKP496	AmpR; NeoR; pcDNA3.0-based plasmid encoding flag-DHFR-ha-Ub-MCS-flag under the control of CMV promoter. MCS has SacII, EcoRI, XhoI, ClaI and EcoRV unique cloning sites.	(23)
pKP536	Amp^R; Neo^R; pcDNA3.0-based plasmid encoding ^{f}DHFR-Ub^{K48R}-Leu28-hCapn1^f under the control of T7 or CMV promoter	This study
pKP537	Amp^R; Neo^R; pcDNA3.0-based plasmid encoding ^{f}DHFR-Ub^{K48R}-Val28-Capn2^f under the control of T7 or CMV promoter	This study
pKP564	Amp^R; Neo^R; pcDNA3.0-based plasmid encoding ^{f}DHFR-Ub^{K48R}-Tyr937-mGrm1^f under the control of T7 or CMV promoter	This study
pKP565	Amp^R; Neo^R; pcDNA3.0-based plasmid encoding ^{f}DHFR-Ub^{K48R}-Val937-mGrm1^f under the control of T7 or CMV promoter	This study
pKP566	Amp^R; Neo^R; pcDNA3.0-based plasmid encoding ^{f}DHFR-Ub^{K48R}-Arg181-mIgfpb2^f under the control of T7 or CMV promoter	This study
pKP567	Amp^R; Neo^R; pcDNA3.0-based plasmid encoding ^{f}DHFR-Ub^{K48R}-Val181-m Igfpb2^f under the control of T7 or CMV promoter	This study
pKP568	Amp^R; Neo^R; pcDNA3.0-based plasmid encoding ^{f}DHFR-Ub^{K48R}-Phe1279-mGluN2a^f under the control of T7 or CMV promoter	This study
pKP569	Amp^R; Neo^R; pcDNA3.0-based plasmid encoding ^{f}DHFR-Ub^{K48R}-Val1279-mGluN2a^f under the control of T7 or CMV promoter	This study
pKP574	Amp^R; Neo^R; pcDNA3.0-based plasmid encoding ^{f}DHFR-Ub^{K48R}-Lys609-mIca512^f under the control of T7 or CMV promoter	This study
pKP575	Amp^R; Neo^R; pcDNA3.0-based plasmid encoding ^{f}DHFR-Ub^{K48R}-Val609-mIca512^f under the control of T7 or CMV promoter	This study
pKP576	Amp^R; Neo^R; pcDNA3.0-based plasmid encoding ^{f}DHFR-Ub^{K48R}-Arg103-mAnkrd2^f under the control of T7 or CMV promoter	This study
pKP577	Amp^R; Neo^R; pcDNA3.0-based plasmid encoding ^{f}DHFR-Ub^{K48R}-Val103-mAnkrd2^f under the control of T7 or CMV promoter	This study
pKP578	Amp^R; Neo^R; pcDNA3.0-based plasmid encoding ^{f}DHFR-Ub^{K48R}-Asp143-mCapns1^f under the control of T7 or CMV promoter	This study
pKP579	Amp^R; Neo^R; pcDNA3.0-based plasmid encoding ^{f}DHFR-Ub^{K48R}-Val143-mCapns1^f under the control of T7 or CMV promoter	This study
pKP582	AmpR; NeoR; pcDNA3.0-based plasmid encoding flag-lacZ$^{25\text{-}119}$-DHFR-ha-Ub-MCS-flag under the control of CMV promoter. MCS has SacII, EcoRI, XhoI, ClaI and EcoRV unique cloning sites.	This study
pKP583	Amp^R; Neo^R; pcDNA3.0-based plasmid encoding ^{f}DHFR-Ub^{K48R}-Glu16-mBak^f under the control of T7 or CMV promoter	This study
pKP584	Amp^R; Neo^R; pcDNA3.0-based plasmid encoding ^{f}DHFR-Ub^{K48R}-Val16-mBak^f under the control of T7 or CMV promoter	This study
pKP599	Amp^R; Neo^R; pcDNA3.0-based plasmid encoding full length ^{f}Ica512^f under the control of T7 or CMV promoter	This study
pKP600	Amp^R; Neo^R; pcDNA3.0-based plasmid encoding Lys609Val mutant of full length ^{f}Ica512^f (^{f}Ica512^f-K609V) under the control of T7 or CMV promoter	This study
pKP631	Amp^R; Neo^R; pcDNA3.0-based plasmid encoding ^{f}DHFR-Ub^{K48R}-Lys10-hCapn2^f under the control of T7 or CMV promoter	This study
pKP632	Amp^R; Neo^R; pcDNA3.0-based plasmid encoding ^{f}DHFR-Ub^{K48R}-Val10-hCapn2^f under the control of T7 or CMV promoter	This study
pJO386	Amp^R; Neo^R; pcDNA3.0-based plasmid encoding ^{f}DHFR-Ub^{K48R}-Arg1091-mAtb2b2^f under the control of T7 or CMV promoter	This study
pJO387	Amp^R; Neo^R; pcDNA3.0-based plasmid encoding ^{f}DHFR-Ub^{K48R}-Val1091-mAtb2b^f under the control of T7 or CMV promoter	This study
pJO425	Amp^R; Neo^R; pcDNA3.0-based plasmid encoding flag-lacZ$^{25\text{-}119}$-DHFR-Ub^{K48R}-Arg91-mc-Fos^f under the control of T7 or CMV promoter	This study

Table S1. Cont.

Plasmid	Description	Source or reference
pJO426	Amp^R; Neo^R; pcDNA3.0-based plasmid encoding flag-lacZ$^{25\text{-}119}$-DHFR-Ub^{K48R}-Val91-mc-Fos^f under the control of T7 or CMV promoter	This study
pJO427	Amp^R; Neo^R; pcDNA3.0-based plasmid encoding flag-lacZ$^{25\text{-}119}$-DHFR-Ub^{K48R}-Glu51-mIκBα^f under the control of T7 or CMV promoter	This study
pJO428	Amp^R; Neo^R; pcDNA3.0-based plasmid encoding flag-lacZ$^{25\text{-}119}$-DHFR-Ub^{K48R}-Val51-mIκBα^f under the control of T7 or CMV promoter	This study

Table S2. Primers used in this study

Primer	Primer's sequence
706	TTTTTTCTAGACTAACCTTTGTCGTCATCGTC
757	GGGCCGCGGAGGACGGATCCAGACACAGATCCGCGTCGTGAAG
758	GGGCCGCGGAGGAGTTATCCAGACACAGATCCGCGTCGTGAAG
759	CGCCGATATCCATGGACATAGCCATAAGCGACGTCTCCAGGCTGTGGATGGGGCT
760	GGGCCGCGGAGGAAGAGCGCCCCATCCTTACGGACTCCCCACC
761	GGGCCGCGGAGGAGTTGCGCCCCATCCTTACGGACTCCCCACC
762	CGCCATCGATCATAGCCATCAGGGCCAGCAGCGTGGGTGAGCTCAGGGA
763	GGGCCGCGGAGGAGAGATCCGCCTGCAGCCGCAGGAGGCGCCG
764	GGGCCGCGGAGGAGTTATCCGCCTGCAGCCGCAGGAGGCGCCG
765	CGCCATCGATCATGGACATAGCCATTAATGTCAGACGCTGGCCTCCAAACACACA
1490	TTTTAATCGATGTGATGATGGTGGTGGTGATGTGCAAACATGGTCAGCTGCAA
1510	AAAAACCGCGGAGGACTGGGCCGCCATGAGAATGCC
1511	AAAAACCGCGGAGGAGTTGGCCGCCATGAGAATGCC
1512	GGGAGCACCGCTGGGGGCTGCCG
1513	CGGCAGCCCCCAGCGGTGCTCCC
1570	AAAAACCGCGGAGGACGTGAGATCATTGATGTGGGTGGGA
1571	AAAAACCGCGGAGGAGTTGAGATCATTGATGTGGGTGGGA
1572	TTTTAATCGATCTGGGCTGGTATAGGCTGAGGTG
1576	AAAAACCGCGGAGGAGACACTTGTCGGAGCATGGTGGCCG
1577	AAAAACCGCGGAGGAGTTACTTGTCGGAGCATGGTGGCCG
1578	TTTTAATCGATGGAATACATAGTCAGCTGCAGCCACT
1579	AAAAACCGCGGAGGATACCAAGGCTCTGGCAAGAGTCTGA
1580	AAAAACCGCGGAGGAGTTCAAGGCTCTGGCAAGAGTCTGA
1581	TTTTAATCGATCAGAGTGGAAGAGCTTTGCTTGTAG
1582	AAAAACCGCGGAGGACGGCAGATGGGCAAGGGTGCCAAAC
1583	AAAAACCGCGGAGGAGTTCAGATGGGCAAGGGTGCCAAAC
1584	TTTTAATCGATCTGCACACTTTGGGCATGGGC
1585	AAAAACCGCGGAGGATTCCAGAAGAACAAGCTAAAGATTAATCGACA
1586	AAAAACCGCGGAGGAGTTCAGAAGAACAAGCTAAAGATTAATCGACA
1587	TTTTAATCGATGACATCAGATTCAATACTAGGCATTTT
1591	AAAAACCGCGGAGGAAAGGAGCGCCTGGCAGCGCTGGGGC
1592	AAAAACCGCGGAGGAGTTGAGCGCCTGGCAGCGCTGGGGC
1593	TTTTAATCGATCTGGGGCAGGGCCTTGAGGAT
1597	TCCTGGTACTCAAAAGTAGTGTCACCATGGGCCCCCTCCGGCCCCAGCGCTGCCAGGCGC
1598	GGTGACACTACTTTTGAGTACCAGGACC
1605	ACCCAAGCTTATGGACTACAAGGACGACGATGACAAGGGTGCACGACAGGTTTCCCGACT
1606	TTAAAGGATCCATTCTCCGTGGGAACAAACGG
1610	AAAAACCGCGGAGGAGAGTCCCCGTCCCCTTCTGAACA
1611	AAAAACCGCGGAGGAGTTTCCCCGTCCCCTTCTGAACA
1612	TTTTAATCGATAACCACGCTGGTAGACGTACAGG
1632	AAAAAAAGCTTAGGAGGCCACCATGAGGCGCCCGCGGCGGCC
1633	ACCTTTGTCGTCATCGTCTTTGTAGTCGGCACTGATGGCGCTGCAGCCCCCGG
1634	CGACTACAAAGACGATGACGACAAAGGTCACGGCTGTCTGTTTGACCGCAG
1635	GTACTTCCTCCTCATGGCCCTCTGAAG
1636	CTTCAGAGGGCCATGAGGAGGAAGTAC
1637	TTTTAAGCGCTGCCAGGCGCTCCTTATCCCGCTGTCTCGAATG
1638	TTTTAAGCGCTGCCAGGCGCTCAACATCCCGCTGTCTCGAATG
1731	AAAAACCGCGGAGGAAAGGACCGGGAGGCGGCCGAGGGGCT
1732	AAAAACCGCGGAGGAGTTGACCGGGAGGCGGCCGAGGGGCT
1733	GATGGCCTCCGAGTCAGCGGCGCTGGTGATG
1734	CATCACCAGCGCCGCTGACTCGGAGGCCATC
1735	TTCCTGCAACCTCCAGCGGTGGAGCCCCGC
1736	GCGGGGCTCCACCGCTGGAGGTTGCAGGAA
1737	CTAACCTTTGTCGTCATCGTCTTTGTAGTCAAGTACTGAGAAACAGAGCCAAGA